NUCLEAR SCIENCE AND TECHNIQUES **2**, S20511 (2015)

Flavor-mixing induced by the mismatched vector interactions at finite μ_I*

ZHANG Zhao (张昭)† and SU Hai-Peng (苏海鹏)
School of Mathematics and Physics, North China Electric Power University, Beijing 102206, China
(Received January 15, 2015; accepted in revised form February 7, 2015; published online April 20, 2015)

The relation between the vector-isoscalar and vector-isovector interactions in the two-flavor Nambu-Jona-Lasinio (NJL) model is investigated under the different constraints from QCD. We demonstrate that the flavor-mixing can be induced by the mismatched vector-isoscalar and vector-isovector interactions at finite baryon chemical potential μ and isospin chemical potential μ_I. The effect of this non-anomaly flavor-mixing on the possible separate chiral transitions at nonzero μ_I is studied under the assumption of the effective restoration of $U(1)_A$ symmetry. We find that for the weak isospin asymmetry, the two separate phase boundaries found previously can be converted into one only if the vector-isovector coupling g_v^v is significantly stronger than the vector-isoscalar one g_v^s without the axial anomaly.

Keywords: Chiral phase transition, QCD critical point, Flavor-mixing, Isospin chemical potential

DOI: 10.13538/j.1001-8042/nst.26.S20511

I. INTRODUCTION

Plotting the map of QCD phase diagram at finite temperature T and quark chemical potential μ has attracted growing interests. Especially, a chiral critical endpoint is predicted by some model studies, which separates the crossover and the first order phase transition. Currently, the lattice QCD computations at finite density still struggle in a limited range of μ [1]. So the existence and location of the critical endpoint are still under debate due to the lack of reliable theoretical methods for the non-perturbative dense QCD. Theoretically, fluctuations of conserved charges, such as net-baryon, net-charge and net-strangeness, are predicted to be sensitive to the correlation length of the system [2–4] and directly connected to some susceptibilities [5, 6]. Thus, the experimental data related to these quantities can serve as powerful tools to probe the critical endpoint in heavy-ion collisions: the search for such a point is ongoing at RHIC (BES) [7–9] and will be performed in the future facilities in GSI (FAIR) and JINR (NICA). Moreover, unconventional multiple chiral critical endpoints are also proposed: it is found in [10, 11] that the finite isospin chemical potential μ_I may lead to two critical endpoints; when considering the color superconductivity (CSC), the low-temperature critical endpoint(s) may appear due to the interplay between the chiral and diquark condensates [12–17].

Besides T and μ, the $U(1)_A$ anomaly may impact the QCD phase transition significantly [18]. This point has been confirmed in model studies or Ginzberg-Landau analyses, where the $U(1)_A$ anomaly is usually incorporated by introducing the Kabayashi-Maskawa-'t Hooft (KMT) interaction [19–21]. The KMT interaction explicitly breaks the $U(1)_A$ symmetry and gives rise to the flavor-mixing among light quarks: the dynamical mass of u quark may contain contributions from both d and s quark condensates; the diquark condensate for u-d pairing at moderate or high baryon density may make contribution to the s quark mass. Consequently, the $U(1)_A$ anomaly may affect not only the properties of the traditional critical endpoint [22], but also that of the unconventional one: the separation of chiral transition due to finite μ_I [10, 11] may be removed by the anomaly flavor-mixing [23]; a new critical endpoint at low temperature could be induced in the presence of the color flavor locking (CFL) CSC [13].

However, the recent lattice calculations indicate that the $U(1)_A$ symmetry may be restored obviously near and above T_c for zero μ [24, 25]. The effective restoration of the $U(1)_A$ symmetry would influence the universality class and critical properties of the chiral transition [26]. Phenomenologically, the model studies suggest that the properties of the conventional critical endpoint are quite sensitive to the degree of $U(1)_A$ restoration [22]. Moreover, if the anomaly related flavor-mixing is very weak near the phase boundary, the two critical endpoints due to the isospin asymmetry [10, 11] could still be possible due to the decouple of light quarks.

On the other hand, it is also probable that the non-anomaly flavor-mixing can be induced by other ingredients of QCD, especially under some condition. The main purpose of this work is to study the possible non-anomaly flavor-mixing of light quarks and its effect on the chiral phase transition under the isospin asymmetry. In particular, we will focus on the fate of the two critical endpoints due to the separate chiral transitions found in [10, 11] with the assumption of the effective restoration of $U(1)_A$ symmetry near the phase boundary.

Our starting point is the four-quark vector interactions with different coupling strengths in the isovector and isoscalar channels. The effect of vector interactions on the chiral transition has been extensively studied in the NJL-type model of QCD. A well-known result is that the chiral transition at finite μ is weakened by the vector-isoscalar interaction $g_v^s(\bar{\psi}\gamma_\mu\psi)^2$ and the critical point disappears for strong g_v^s [12, 15, 22, 27]. It is also found that the g_v^s in a proper range can lead to the new low-temperature critical endpoint(s) [12] when considering the two-flavor CSC, especially with the constraint of electric-charge neutrality [15, 17]. In general, g_v^s and the isovector coupling g_v^v are independent coupling constants un-

* Supported by the National Natural Science Foundation of China (No. 11275069)
† Corresponding author, zhaozhang@pku.org.cn

der the chiral symmetry. In the literature, the non-anomaly flavor-mixing due to the mismatched vector interactions in the vacuum has been discussed in Ref. [28] based on a three-flavor NJL model. We extend such a work to finite T and μ to study the effect of the non-anomaly flavor-mixing on the chiral transition with isospin asymmetry.

II. EXTENDED NJL-TYPE MODEL WITH MISMATCHED VECTOR INTERACTIONS

A. The general four-quark interaction model with mismatched vector interactions under the chiral symmetry

We start with the following Lagrangian of four-quark interaction model for two-flavor QCD

$$\mathcal{L}^{(4)} = \mathcal{L}^{(4)}_{\rm sym} + \mathcal{L}^{(4)}_{\rm det}, \tag{1}$$

with

$$\begin{aligned}\mathcal{L}^{(4)}_{\rm sym} = & g_{s1}\sum_{a=0}^{3}[(\bar\psi\tau^a\psi)^2 + (\bar\psi\tau^a i\gamma_5\psi)^2] \\ & - g_{v2}\sum_{a=0}^{3}[(\bar\psi\tau^a\gamma_\mu\psi)^2 + (\bar\psi\tau^a\gamma_\mu\gamma_5\psi)^2] \\ & - g_{v3}[(\bar\psi\tau^0\gamma_\mu\psi)^2 + (\bar\psi\tau^0\gamma_\mu\gamma_5\psi)^2] \\ & - g_{v4}[(\bar\psi\tau^0\gamma_\mu\psi)^2 - (\bar\psi\tau^0\gamma_\mu\gamma_5\psi)^2],\end{aligned} \tag{2}$$

and

$$\begin{aligned}\mathcal{L}^{(4)}_{\rm det} &= g_{s2}\{det[\bar\psi(1-\gamma_5)\psi] + h.c.\} \\ &= g_{s2}[(\bar\psi\psi)^2 - (\bar\psi\vec\tau\psi)^2 - (\bar\psi i\gamma_5\psi)^2 + (\bar\psi\vec\tau i\gamma_5\psi)^2],\end{aligned} \tag{3}$$

where τ^0, and $\vec\tau$ refer to the unit matrix and Pauli matrices in the flavor space, respectively. The former term $\mathcal{L}^{(4)}_{\rm sym}$ in (1) is the general Fierz-invariant form of the four-quark interactions in color-singlet channels which respecting the global flavor symmetries of $SU(2)_V\otimes SU(2)_A\otimes U(1)_V\otimes U(1)_A$ [29]. The latter one $\mathcal{L}^{(4)}_{\rm det}$ is the KMT interaction induced by the gauge configurations of instanton and anti-instanton [19, 20], which only possesses the $SU(2)_V\otimes SU(2)_A\otimes U(1)_V$ global flavor symmetries.

As mentioned, we will focus on the flavor-mixing arising from the mismatched vector interactions at finite density. We see that three of four independent coupling constants in $\mathcal{L}^{(4)}_{\rm sym}$ are related to the vector and axial vector interactions. Generally, the nozero sum $g_{v3} + g_{v4}$ implies that the vector coupling strength in the isovector channel is different from that in the isoscalar one. Similarly, the non-vanishing $g_{v3} - g_{v4}$ indicates the axial-vector interactions are also mismatched in the isovector and isoscalar channels. How the vector coupling difference gives rise to the non-anomaly flavor-mixing at finite density will be detailed in next section.

The axial-vector interaction may be responsible for the deviation of the chiral magnetic effect in the recent lattice calculation compared to the analytic formula, as proposed in Ref. [30]. Here we mainly study the chiral phase transition in the MFA, the axial-vector interactions in Lagrangian (1) will be ignored. Thus we only consider the the following effective Lagrangian,

$$\begin{aligned}\mathcal{L}^{(4)}_{\rm eff} = & g_{s1}\sum_{a=0}^{3}[(\bar\psi\tau^a\psi)^2 + (\bar\psi\tau^a i\gamma_5\psi)^2] \\ & + g_{s2}[(\bar\psi\psi)^2 - (\bar\psi\vec\tau\psi)^2 - (\bar\psi i\gamma_5\psi)^2 + (\bar\psi\vec\tau i\gamma_5\psi)^2] \\ & - g^s_v(\bar\psi\gamma_\mu\psi)^2 - g^v_v(\bar\psi\vec\tau\gamma_\mu\psi)^2,\end{aligned} \tag{4}$$

where the independent coupling constants are reduced to four.

B. Unequal vector coupling constants in the mean field Hartree-Fork approximation

Here we stress that the vector coupling difference in the MFA can also arise from a very popular version of the NJL model [29],

$$\begin{aligned}\mathcal{L}^{(4)} = & g_{s1}\sum_{a=0}^{3}[(\bar\psi\tau^a\psi)^2 + (\bar\psi\tau^a i\gamma_5\psi)^2] \\ & + g_{s2}[(\bar\psi\psi)^2 - (\bar\psi\vec\tau\psi)^2 - (\bar\psi i\gamma_5\psi)^2 + (\bar\psi\vec\tau i\gamma_5\psi)^2] \\ & - g_{v}\sum_{a=0}^{3}[(\bar\psi\tau^a\gamma_\mu\psi)^2 + (\bar\psi\tau^a\gamma_\mu\gamma_5\psi)^2],\end{aligned} \tag{5}$$

in which only one vector coupling g_v is adopted. In the Hartree approximation, there is no difference between the coupling strengths of the two vector interactions at the mean field level for Lagrangian (5).

However, the effective vector couplings (in the sense of direct interaction) in the isoscalar and isovector channels will differ from each other if the Fock contribution is also considered. For a four-fermion interaction, the Fock contribution can be easily evaluated according to its Fierz transformation [29]. Taking into account the exchange terms, the effective direct four-quark interactions of the Lagrangian (5) take the following form

$$\begin{aligned}\mathcal{L}^{(4)}{}_{\text{eff-direct}} &= \mathcal{L}^{(4)} + \mathcal{L}^{(4)}_{\rm Fock} \\ &= (g_{s1} + g_{s2} + \frac{g_{s2}}{2N_c})[(\bar\psi\psi)^2 + (\bar\psi i\gamma_5\vec\tau\psi)^2] \\ &+ (g_{s1} - g_{s2} - \frac{g_{s2}}{2N_c})[(\bar\psi\vec\tau\psi)^2 + (\bar\psi i\gamma_5\psi)^2] \\ &- g_v\sum_{a=0}^{3}[(\bar\psi\tau^a\gamma_\mu\psi)^2 + (\bar\psi\tau^a\gamma_\mu\gamma_5\psi)^2] \\ &- (\frac{g_v}{N_c} + \frac{1}{2}\frac{g_{s1}}{N_c})(\bar\psi\tau^0\gamma_\mu\psi)^2 \\ &- (\frac{g_v}{N_c} - \frac{1}{2}\frac{g_{s1}}{N_c})(\bar\psi\tau^0\gamma_\mu\gamma_5\psi)^2,\end{aligned} \tag{6}$$

where N_c is the color number of the quarks. The effective Lagrangian (6) clearly shows that the exchange terms give rise to the vector coupling difference in the Hartree-Fock approximation (HFA), which is at the order of $O(1/N_c)$ compared to g_{s1} and g_v. Note that the similar result in a three-flavor NJL model has been given in [28].

If both g_v and g_{s1} in (5) originate from the color current-current interaction $g(\bar{\psi}\gamma_\mu\lambda_c^a\psi)^2$, they fulfill the relation $g_v = g_{s1}/2$ according to the Fierz transformation. In this case, the vector coupling difference shown in (6) becomes

$$\delta g_v = g_v^s - g_v^v = \frac{2}{N_c} g_v = \frac{g_{s1}}{N_c}. \tag{7}$$

This equation indicates that g_v^s in (4) may be larger than g_v^v and their difference is considerable compared to g_v or g_{s1} for $N_c = 3$.

C. Constraints on the vector interactions from the lattice chiral curvatures

Even Eq. (7) implies that the coupling g_v^v is weaker than g_v^s, it is also possible that g_v^v may be stronger than g_v^s. This can be understood from the curvature difference for the chiral phase transition at finite baryon and isospin chemical potentials obtained in recent lattice calculations [31].

For small baryon and isospin densities, the chemical potential dependence of the pseudo-critical temperature for the chiral crossover can be expressed as

$$T_c(\mu_q, \mu_i) = T_c + A_q\mu_q^2 + B_i\mu_i^2 + O(\mu_{q/i}^4, \mu_q^2\mu_i^2), \tag{8}$$

where T_c is the chiral pseudo-critical temperature at zero quark chemical potential (In this subsection, μ_q and μ_i are used to refer to the quark baryon and isospin chemical potentials, respectively). Notice that $T_c(\mu_q, \mu_i)$ is an even function of $\mu_{q/i}$ [32]. So at the order of $\mu_{q/i}^2$, we can expand $T_c(\mu_{q/i}^2)$ as

$$T_c(\mu_{q/i}^2) = T_c(1 - \kappa_{q/i}\frac{\mu_{q/i}^2}{T_c^2}), \tag{9}$$

where the two chiral curvatures are defined as

$$\kappa_{q/i} = -T_c\frac{dT_c(\mu^2)}{d\mu_{q/i}^2}|_{\mu=0}. \tag{10}$$

The lattice QCD simulation in [31] suggests that the curvature κ_q is about 10% greater than κ_i.

Recently, the role of g_v^s on the determination of κ_q has been studied in a Polyakov-loop enhanced three-flavor NJL model [22]. It is found that κ_q decreases with g_v^s and to reproduce the lattice κ_q the g_v^s must keep relatively larger value compared to g_s. The authors of Ref. [22] then propose the lattice κ_q can be used as a useful constraint on g_v^s.

We can directly extend this idea to determine κ_i by replacing μ_q with μ_i. As will be demonstrated in the next section, the coupling g_v^v influences the curvature κ_i in the similar way as g_v^s does on κ_q. In particular, κ_i and κ_q obtained at the MFA of the two-flavor NJL model will take the same value for $g_v^v = g_v^s$. In other words, the lattice curvature difference between κ_i and κ_q can be regarded as an useful evidence for the unequal vector coupling strengths.

Since the two-flavor lattice calculation in [31] indicates that κ_i is less than κ_q, we thus infer that g_v^v may be larger than g_v^s near the chiral phase boundary for zero and small quark chemical potential. Following the spirit of Ref. [22], our numerical study suggests that g_v^v is about 10% larger than g_v^s near T_c according to the lattice curvatures in [31]. Note that this conclusion is quite different from the estimation given in (7).

D. Constraints on the vector interactions from the couplings of vector mesons to nucleons and lattice susceptibilities

In Ref. [33], it is argued that the ratio of the couplings of ω and ρ mesons to nucleons can be used as a constraint on the vector coupling difference. In the chirally broken phase, the empirical value for this ratio is given by $g_{\omega NN}/g_{\rho NN} \simeq 3$, whereas in the chirally symmetric phase it is expected to be one. It is then proposed that the ratio g_v^v/g_v^s is located in the range from 1/3 to 1.

In addition, another quite similar estimation is given in Ref. [34], where the vector coupling difference is expressed as the function of two susceptibilities χ_q and χ_I under some assumptions. Using the lattice data for these susceptibilities as input, it is found that g_v^v is always less than g_v^s: their difference is quite large below T_c which approaches zero rapidly above T_c for zero chemical potential.

All the arguments given in the above subsections suggest that the vector interactions are repulsive (namely, g_v^s and g_v^v are all positive), but the relation between the g_v^s and g_v^v remains uncertain. In the following study, g_v^s and g_v^v in (4) will be treated as the free parameters due to these uncertainties.

III. VECTOR-INTERACTION INDUCED FLAVOR-MIXING AND THE THERMAL DYNAMICAL POTENTIAL AT FINITE BARYON AND ISOSPIN CHEMICAL POTENTIALS

In this section, we shall demonstrate that the vector coupling difference can lead to non-anomaly flavor-mixing at finite baryon and isospin densities.

The full Lagrangian of two-flavor NJL model with the interaction (4) reads

$$\mathcal{L} = \bar{\psi}\left(i\partial_\mu\gamma^\mu + \gamma_0\hat{\mu} - \hat{m}_0\right)\psi + \mathcal{L}_{\text{eff}}^{(4)}, \tag{11}$$

where the quark chemical potentials are introduced and $\hat{m}_0 = \text{diag}(m_u, m_d)$ is the current quark matrix. We shall adopt the isospin symmetric quark masses with $m_u = m_d \equiv m_0$. The $\hat{\mu}$ in the Lagrangian (11) is the matrix of the quark chemical potentials which takes form

$$\hat{\mu} = \begin{pmatrix} \mu_u & \\ & \mu_d \end{pmatrix} = \begin{pmatrix} \mu - \mu_I & \\ & \mu + \mu_I \end{pmatrix}, \tag{12}$$

with

$$\mu = \frac{\mu_u + \mu_d}{2} = \frac{\mu_B}{3} \quad \text{and} \quad \mu_I = \frac{\mu_u - \mu_d}{2} = \frac{\delta\mu}{2}. \tag{13}$$

In (13), μ_B (μ_I) is the baryon (isospin) chemical potential. Note that the definition of the isospin chemical potential in

the quark level is different from that in the nucleon level. For more details on the role of isospin symmetry energy in nuclear matter, the reader can refer to [35–38] and references therein.

At finite densities, the quark chemical potentials are shifted by the vector interactions. Here we use μ' to denote the modified quark chemical potential. Note that the u quark density is different from the d quark one under the isospin asymmetry. The shifted quark chemical potentials take the form

$$\begin{aligned}\mu'_{u(d)} &= \mu_{u(d)} - 2g_v^s(\rho_u + \rho_d) - 2g_v^v(\rho_{u(d)} - \rho_{d(u)}) \\ &= \mu_{u(d)} - 2(g_v^s + g_v^v)\rho_{u(d)} - 2(g_v^s - g_v^v)\rho_{d(u)},\end{aligned} \tag{14}$$

or

$$\mu' = \mu - 2g_v^s(\rho_u + \rho_d), \quad \mu'_I = \mu_I - 2g_v^v(\rho_u - \rho_d) \tag{15}$$

where

$$\rho_{u(d)} = \langle \psi^\dagger_{u(d)} \psi_{u(d)} \rangle, \tag{16}$$

is the u (d) quark number density. Eq. (14) clearly shows that due to the vector coupling difference, not only ρ_u but also ρ_d give contribution to the effective chemical potential of u quark, and vise versa. This implies that the flavor-mixing arises due to the vector interaction. As mentioned, this mixing has nothing to do with the axial anomaly. The modified chemical potentials can also be rearranged as Eq. (15), which indicates that μ and μ_I are shifted by the isoscalar and isovector vector interactions, respectively.

Formally, the non-anomaly flavor-mixing shown in (14) for the modified chemical potentials is quite similar to the anomaly flavor-mixing for the constituent quark masses induced by the instantons, namely:

$$M_{u(d)} = m_0 - 4g_{s1}\phi_{u(d)} - 4g_{s2}\phi_{d(u)}, \tag{17}$$

where

$$\phi_{u(d)} = \langle \bar{\psi}_{u(d)} \psi_{u(d)} \rangle, \tag{18}$$

is the u (d) quark condensate.

Using the conventional technique, the mean field thermal dynamical potential of the Lagrangian (11) is expressed as

$$\begin{aligned}&\Omega(T, \mu_u, \mu_d) = \\ &\sum_{f=u,d} \Omega_0(T, \mu'_f; M_f) + 2g_{s1}(\phi_u^2 + \phi_d^2) + 4g_{s2}\phi_u\phi_d \\ &- (g_v^s + g_v^v)(\rho_u^2 + \rho_d^2) - 2(g_v^s - g_v^v)\rho_u\rho_d,\end{aligned} \tag{19}$$

where $\Omega_0(T, \mu'_f; M_f)$ is the contribution of a quasi-particle gas of the flavor f which takes the form

$$\begin{aligned}&\Omega_0(T, \mu'_f; M_f) = \\ &- 2N_c T \int \frac{d^3p}{(2\pi)^3} \Big[\ln[1 + \exp(-(E_f - \mu'_f)/T)] \\ &+ \ln[1 + \exp(-(E_f + \mu'_f)/T)] \Big] \\ &- 2N_c \int \frac{d^3p}{(2\pi)^3} E_f \theta(\Lambda^2 - \vec{p}^2),\end{aligned} \tag{20}$$

with the quasi-particle energy $E_f = \sqrt{\vec{p}^2 + M_f^2}$. The Λ in Eq. (20) is the parameter of three-momentum cutoff in the NJL model. We see that besides the modified chemical potential μ'_f, the flavor-mixing due to the vector coupling difference is also explicitly demonstrated in Eq. (19) via the direct coupling between ρ_u and ρ_d.

Minimizing the thermal dynamical potential Eq. (19), the motion equations for the mean fields ϕ_u, ϕ_d, ρ_u and ρ_d are determined through the coupled equations

$$\frac{\partial\Omega}{\partial\phi_u} = 0, \quad \frac{\partial\Omega}{\partial\phi_d} = 0, \quad \frac{\partial\Omega}{\partial\rho_u} = 0, \quad \frac{\partial\Omega}{\partial\rho_d} = 0. \tag{21}$$

This set of equations is then solved for the fields ϕ_u, ϕ_d, ρ_u and ρ_d as functions of the temperature and chemical potentials.

IV. FATE OF THE SEPARATE CHIRAL TRANSITIONS WITH NON-ANOMALY FLAVOR-MIXING

As mentioned, the separate chiral transitions due to finite μ_I [10, 11] can be removed by the flavor-mixing induced by the axial anomaly [23]. Since the instanton density may be suppressed significantly near the phase boundary, we revisit this problem by taking into account the non-anomaly flavor-mixing due to the mismatched vector interactions.

For comparison, we follow the notations in Ref. [23] and introduce two parameters α and g_s which are defined as

$$g_{s1} = (1 - \alpha)g_s, \qquad g_{s2} = \alpha g_s, \tag{22}$$

here α means the ratio of the KMT interaction in the scalar-pseudoscalar channel, which is treated as a free parameter in the following calculations. The other model parameters, namely the current quark mass m_0, the scalar coupling constant g_s and the three-momentum cutoff Λ are all adopted from [23].

A. Fate of separate chiral transitions under the weak isospin asymmetry without the axial anomaly

The role of the mismatched vector interactions on the separation of chiral transition at finite T-μ under the weak isospin asymmetry is investigated by switching off the KMT interaction. We focus on whether the two critical endpoints found previously could be ruled out by the non-anomaly flavor-mixing without the help of the axial anomaly.

We first study the cases for $g_v^v > g_v^s$ with a fixed small coupling $g_v^s = 0.2g_s$ under the weak isospin asymmetry $\delta\mu = -20$ MeV (The typical value of $\delta\mu$ in heavy ion collisions may be within this range, as estimated in [23]) [3]. The T–μ phase diagrams for varied g_v^v are shown in Fig. 1. For

[3] Note that the μ_I defined in [23] corresponds to the $\delta\mu$ in our notations

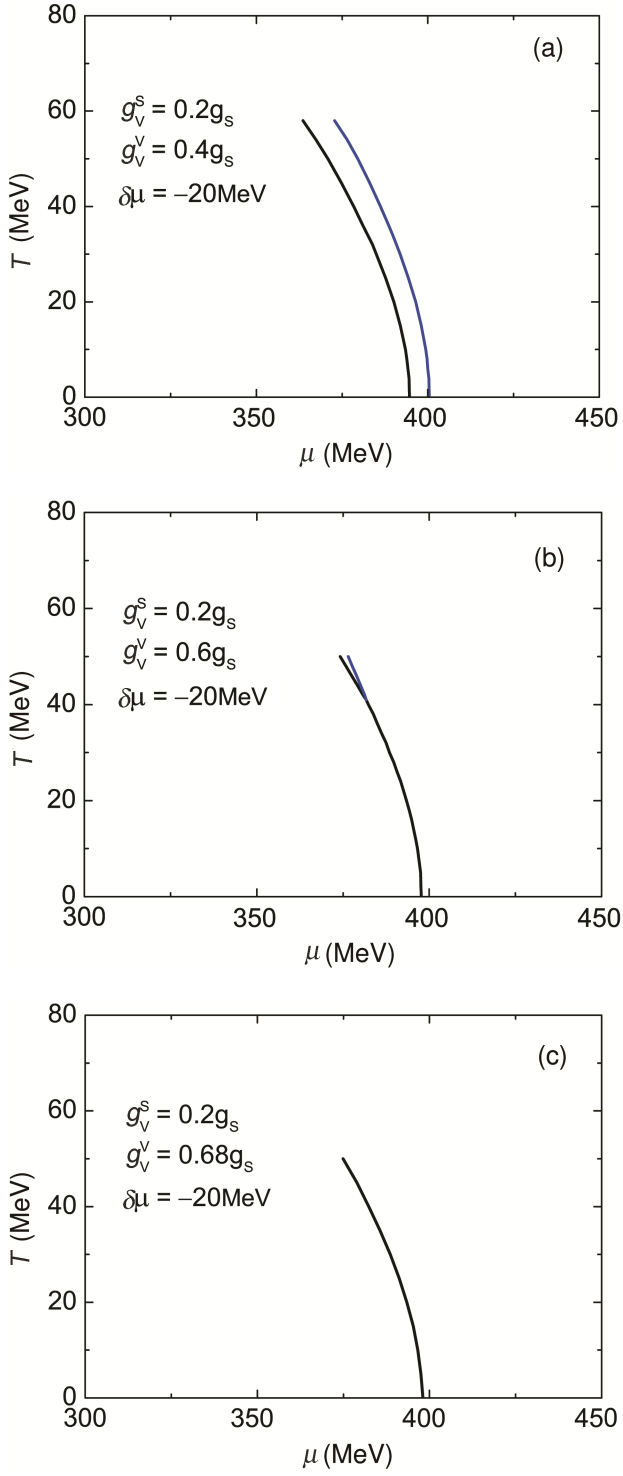

Fig. 1. (Color online) The T-μ phase diagrams for varied vector-isovector coupling g_v^v at $\delta\mu = -20$ MeV without the axial anomaly. The vector-isoscalar coupling g_v^s is fixed as $0.2g_s$. The solid line stands for the first-order chiral boundary.

$g_v^v = 2.0g_v^s$, Fig. 1(a) shows two separate first-order phase boundaries, which correspond to the chiral transitions for the u and d quarks, respectively. For $g_v^v = 0.6g_s$, Fig. 1(b) shows that only one first-order chiral boundary emerges at the low temperature, but it splits into two lines at the relatively higher temperature. So there are still two critical endpoints. Further increasing g_v^v to $0.68g_s$, Fig. 1(c) displays that only one phase boundary appears. So we really observe that the two separate phase boundaries can be changed into one by the non-anomaly flavor-mixing induced by the mismatched vector interactions.

The above calculation for $\delta\mu = -20$ MeV is further extended to a fixed moderate coupling $g_v^s = 0.4g_s$. The phase diagrams for varied g_v^v with $g_v^v > g_v^s$ are shown in Fig. 2, which is still analogous to Fig. 1. In contrast to Fig. 1, a stronger g_v^v is required for the conversion of the two phase transitions into one due to the enlarged g_v^s. Fig. 2 also shows that the chiral transition is first softened and then strengthened with g_v^v. By comparison, the chiral transition is always weakened with the increase of g_v^s.

So for the weak isospin asymmetry, Figs. 1 and 2 show that the chiral transition separation can be removed by the mismatched vector interactions, even without the instanton induced flavor-mixing. Actually, all the two sets of phase diagrams in Figs. 1 and 2 are quite similar to Figs. 2 in Ref. [23] obtained by changing the α. In this sense, the non-anomaly flavor-mixing due to the vector coupling difference plays the similar role as the KMT interaction.

However, Figs. 1 and 2 indicate that g_v^v must be much stronger than g_v^s for turning the two chiral transitions into one: g_v^v is at least twice as strong as g_v^s to remove the separation. Of course, the fate of the separate chiral transitions depends on not only the vector coupling difference, but also the magnitudes of g_v^v and g_v^s. Here we do not show the results for $g_v^v > g_v^s$ with a fixed strong g_v^s since in this case only crossover transition appears.

On the contrary, we do not find the coincidence of the detached phase boundaries for $g_v^v < g_v^s$. In Fig. 3, we show the phase diagrams for $\delta\mu = -20$ MeV with varied g_v^s and fixed coupling $g_v^v = 0.2g_s$. We see that the two separate phase boundaries get farther rather than closer with the increase of $|\delta g_v|$ for $g_v^v < g_v^s$, which is quite different from what shown in Figs. 1 and 2.

The reason can be traced back to Eqs. (14) and (15). First, according to Eq. (15), the $|\mu_I'|$ is explicitly less than the $|\mu_I|$ since the signs of μ_I and $-2g_v^v(\rho_u - \rho_d)$ in μ_I' are different for $g_v^v > 0$. So for $g_v^v > g_v^s$ with a fixed g_v^s, increasing g_v^v implies not only the enhancement of the flavor-mixing but also the reduction of $|\mu_I'|$. This is why the two phase boundaries approach each other with g_v^v, as shown in Figs. 1 and 2. Second, near the left side of the right phase boundary, the ρ_d is remarkably larger than the ρ_u because of the significant suppression of the d quark mass; but around the left side of the left phase boundary, the difference between the ρ_d and ρ_u is relatively small. So for $g_v^s > g_v^v$, the flavor-mixing term $-(g_v^s - g_v^v)\rho_d$ in μ_u' impacts the right phase boundary more significantly in contrast to what the corresponding term $-(g_v^s - g_v^v)\rho_u$ in μ_d' does on the left phase boundary, according to Eq. (14). This is why the right phase boundary moves more rapidly towards the higher μ with g_v^s in contrast to the left one, as shown in Fig. 3.

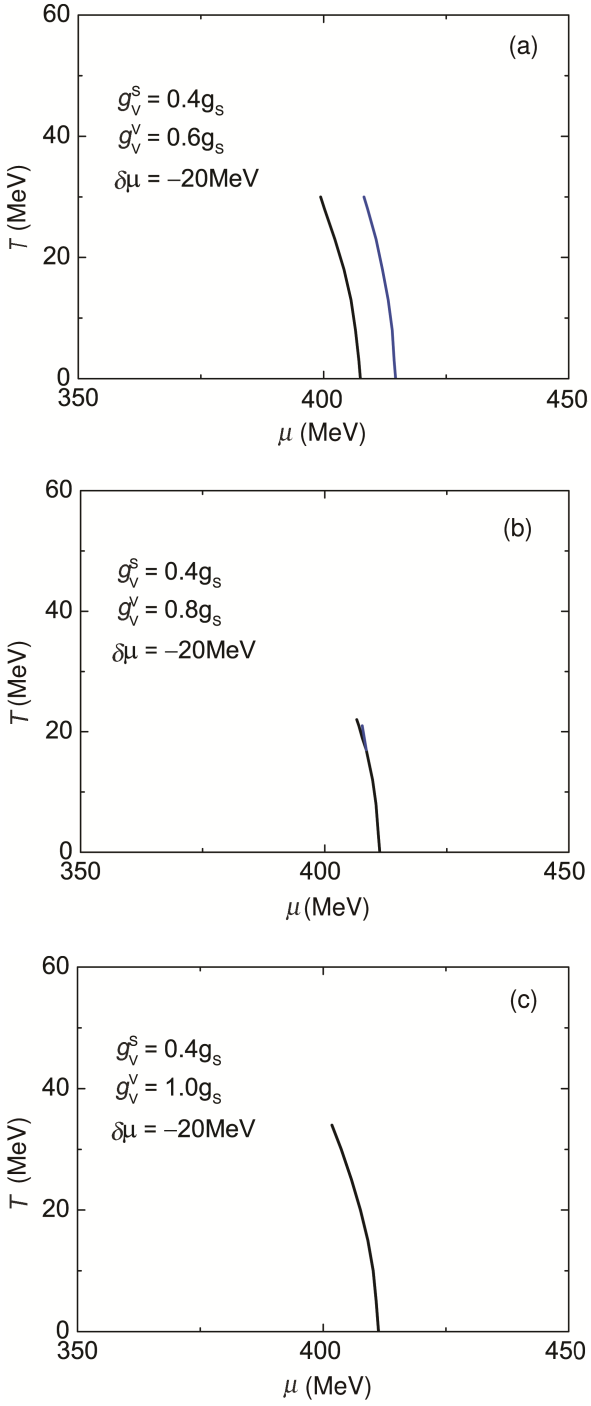

Fig. 2. (Color online) The T-μ phase diagrams for varied vector-isovector coupling g_v^v at $\delta\mu = -20$ MeV without the axial anomaly. The vector-isoscalar coupling is fixed as $g_v^s = 0.4$ (relative to the scalar coupling g_s). The solid line stands for the first-order chiral boundary.

If g_v^s or/and g_v^v are strong enough, the first-order chiral transition will change into crossover and it would be no critical point. Owning to vector interactions, it is possible that one of the two phase boundaries first disappears while the other one still remains with the change of vector interactions (In contrast, the two critical endpoints always appear at the same temperature in Refs. [10, 11]). Such a case is really observed in Fig. 3 for very strong vector interaction $g_v^s = 1.0g_s$. Actually, our numerical study suggests that the emergence of only one critical endpoint via this manner does not require very strong vector interaction when the weak KMT interaction is included.

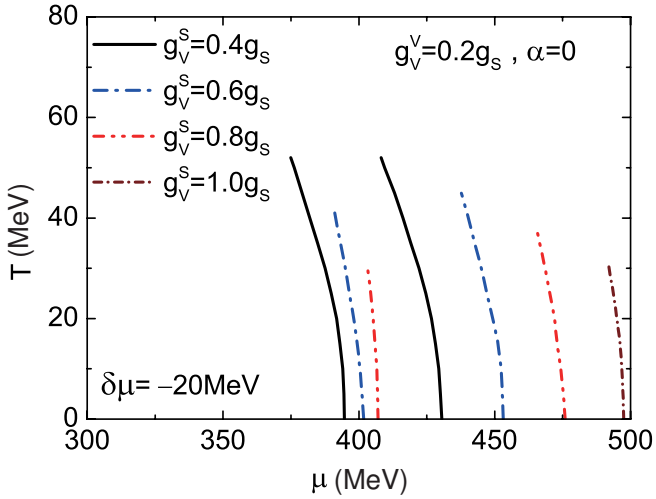

Fig. 3. (Color online) The T-μ phase diagrams for varied vector-isoscalar coupling g_v^s at $\delta\mu = -20$ MeV. The vector-isovector coupling is fixed as $g_v^v = 0.2$ (relative to the scalar coupling g_s). The axial anomaly is ignored. All the lines stand for the first-order chiral boundaries.

Here only the weak isospin asymmetry is considered because $|\mu_I|$ is small in heavy-ion collisions. On the other hand, the quark matter may appear in the core of neutron star. In such a case, the magnitude of the difference between the u and d quark chemical potentials may be as large as 100 MeV due to the constraint of charge neutrality[4]. For the strong isospin asymmetry with a relatively large $|\mu_I|$, we find that the separation of the chiral transition can not be removed by the non-anomaly flavor-mixing without considering the axial anomaly. However, the similar phase diagram as Fig. 3 is still observed for a proper choice of g_v^v and g_v^s.

V. DISCUSSION AND CONCLUSION

We have studied the influence of vector interactions with different coupling constants in the isoscalar and isovector channels on the possible separation of the chiral transition under the isospin asymmetry in a two-flavor NJL model, where the $U(1)_A$ symmetry is assumed to be restored effectively near the phase boundary.

We first show that, besides the argument from the empirically different nucleon and vector-meson couplings [33],

[4] Note that in another case with $|\mu_I| > m_\pi/2$ and vanishing μ, the pion condensation emerges at zero and low tmeperatures[39–41]

the one-gluon exchange type interaction can also give rise to unequal vector interactions with $g_v^s > g_v^v$ in the MFA when including the Fock contribution. On the other hand, by extending the work [24] to finite μ_I, we obtain the quite different vector coupling difference with $g_v^s < g_v^v$ from the constraints of lattice chiral curvatures at zero/small quark chemical potentials. We demonstrate that, similar to the mass-mixing induced by the KMT interaction, the density-mixing of two flavors is produced owning to the mismatched vector interactions.

The role of the non-anomaly flavor-mixing on the chiral phase transition is investigated under the condition with weak isospin asymmetry. We find that to convert the two separate chiral transitions into one, g_v^v must be significantly stronger than g_v^s without the axial anomaly. In this situation, the non-anomaly flavor-mixing induced by vector interactions impacts the separation of chiral phase transitions in the similar way as the anomaly one induced by instantons: the two detached phase boundaries get closer first and then coincide with the enhancement of the flavor-mixing.

Note that recently the Polyakov-Loop extended NJL model has been extensively used to investigate the thermal and dense properties of QCD. We stress that introducing the Polyakov-Loop dynamics does not qualitatively change our main conclusions. In addition, our study can be directly extended to the quark meson model of QCD by incorporating the quark-vector-meson couplings. Especially, it is interesting to investigate the role of the non anomaly flavor-mixing on the possible quark-menson transition in neutron star [42].

[1] Philipsen O. The QCD equation of state from the lattice. Prog Part Nucl Phys, 2013, **70**: 55–107. DOI: 10.1016/j.ppnp.2012.09.003

[2] Stephanov A M. Non-Gaussian fluctuations near the QCD critical point. Phys Rev Lett, 2009, **102**: 032301. DOI: 10.1103/PhysRevLett.102.032301

[3] Athanasiou C, Rajagopal K and Stephanov M. Using higher moments of fluctuations and their ratios in the search for the QCD critical point. Phys Rev D, 2010 **82**: 074008. DOI: 10.1103/PhysRevD.82.074008

[4] Stephanov A M. On the sign of kurtosis near the QCD critical point. Phys Rev Lett,2011, **107**: 052301. DOI: 10.1103/PhysRevLett.107.052301

[5] Gupta S, Luo X, Mohanty B, *et al*. Scale for the phase diagram of quantum chromodynamics. Science, 2011, **332**: 1525-1528. DOI: 10.1126/science.1204621

[6] Gavai V R and Gupta S. Lattice QCD predictions for shapes of event distributions along the freezeout curve in heavy-ion collisions. Phys Lett B, 2011, **696**: 459–C463. DOI: 10.1016/j.physletb.2011.01.006

[7] Mohanty B. STAR experiment results from the beam energy scan program at RHIC. J Phys G Nucl Partic, 2011, **38**: 124023. DOI: 10.1088/0954-3899/38/12/124023

[8] Mitchell T J. The RHIC beam energy scan program: Results from the PHENIX experiment. Nucl Phys A, 2013, **904-905**: 903c–906c. DOI: 10.1016/j.nuclphysa.2013.02.161

[9] Mohanty B. Exploring the QCD phase diagram through high energy nuclear collisions: An overview. The 8th International Workshop on Critical Point and Onset of Deconfinement (CPOD 2013), Napa, California, USA, Mar.11–25, 2013.

[10] Klein B, Toublan D and Verbaarschot M J J. The QCD phase diagram at nonzero temperature, baryon and isospin chemical potentials in random matrix theory. Phys Rev D, 2003, **68**: 014009. DOI: 10.1103/PhysRevD.68.014009

[11] Toublan D and Kogut B J. Isospin chemical potential and the QCD phase diagram at nonzero temperature and baryon chemical potential. Phys Lett B, 2003, **564**: 212–216. DOI: 10.1016/S0370-2693(03)00701-9

[12] Kitazawa M, Koide T, Kunihiro T, *et al*. Chiral and color superconducting phase transitions with vector interaction in a simple model. Prog Theor Phys, 2002, **108**: 929–951. DOI: 10.1143/PTP.108.929

[13] Hatsuda T, Tachibana M, Yamamoto N, *et al*. New critical point induced by the axial anomaly in dense QCD. Phys Rev Lett, 2006, **97**: 122001. DOI: 10.1103/PhysRevLett.97.122001

[14] Zhang Z, Fukushima K and Kunihiro T. Number of the QCD critical points with neutral color superconductivity. Phys Rev D, 2009, **79**: 014004. DOI: 10.1103/PhysRevD.79.014004

[15] Zhang Z and Kunihiro T. Vector interaction, charge neutrality and multiple chiral critical point structures. Phys Rev D, 2009, **80**: 014015. DOI: 10.1103/PhysRevD.80.014015

[16] Zhang Z and Kunihiro T. Roles of axial anomaly on neutral quark matter with color superconducting phase. Phys Rev D, 2011, **83**: 114003. DOI: 10.1103/PhysRevD.83.114003

[17] Kunihiro T, Minami Y and Zhang Z. QCD critical points and their associated soft modes. Prog Theor Phys Suppl, 2010, **186**: 447–454. DOI: 10.1143/PTPS.186.447

[18] Pisarski D R and Wilczek F. Remarks on the chiral phase transition in chromodynamics. Phys Rev D,1984, **29**: 338–341. DOI: 10.1103/PhysRevD.29.338

[19] 't Hooft G. Computation of the quantum effects due to a four-dimensional pseudoparticle. Phys Rev D, 1976, **14**: 3432–3450. DOI: 10.1103/PhysRevD.14.3432

[20] 't Hooft G. How instantons solve the U(1) problem. Phys Rept, 1986, **142**: 357–387. DOI: 10.1016/0370-1573(86)90117-1

[21] Kobayashi M and Maskawa T. Chiral symmetry and η-X mixing. Prog Theor Phys, 1970, **44**: 1422–1424. DOI: 10.1143/PTP.44.1422

[22] Bratovic M N, Hatsuda T and Weise W. Role of vector interaction and axial anomaly in the PNJL modeling of the QCD phase diagram. Phys Lett B, 2013, **719**: 131–135. DOI: 10.1016/j.physletb.2013.01.003

[23] Frank M, Buballa M and Oertel M. Flavor mixing effects on the QCD phase diagram at nonvanishing isospin chemical potential: One or two phase transitions?. Phys Lett B, 2003, **562**: 221–226. DOI: 10.1016/S0370-2693(03)00607-5

[24] Bazavov A, Bhattacharya T, Buchoff I M, *et al*. The chiral transition and $U(1)_A$ symmetry restoration from lattice QCD using domain wall fermions. Phys Rev D, 2012, **86**: 094503. DOI: 10.1103/PhysRevD.86.094503

[25] Cossu G, Aoki S, Fukaya H, *et al*. Finite temperature study of the axial U(1) symmetry on the lattice with overlap fermion formulation. Phys Rev D, 2013, **87**:114514. DOI: 10.1103/PhysRevD.87.114514

[26] Aoki S, Fukaya H and Taniguchi Y. Chiral symmetry restoration, eigenvalue density of Dirac operator and axial U(1)

anomaly at finite temperature. Phys Rev D, 2012, **86**: 114512. DOI: 10.1103/PhysRevD.86.114512
[27] Asakawa M and Yazaki K. Chiral restoration at finite density and temperature. Nucl Phys A,1989, **504**: 668–684. DOI: 10.1016/0375-9474(89)90002-X
[28] Takizawa M, Kunihiro T and Kubodera K. Axial vector matrix elements Of the proton in the Nambu-Jona-Lasinio model. Phys Lett B, 1990, **237**: 242–247. DOI: 10.1016/0370-2693(90)91436-F
[29] Klevansky P K. The Nambu-Jona-Lasinio model of quantum chromodynamics. Rev Mod Phys, 1992, **64**: 649–708. DOI: 10.1103/RevModPhys.64.649
[30] Zhang Z. Correction to the chiral magnetic effect from axial-vector interaction. Phys Rev D, 2012, **85**: 114028. DOI: 10.1103/PhysRevD.85.114028
[31] Cea P, Cosmai L, D'Elia M, *et al*. The critical line of two-flavor QCD at finite isospin or baryon densities from imaginary chemical potentials. Phys Rev D, 2012, **85**: 094512. DOI: 10.1103/PhysRevD.85.094512
[32] D'Elia M and Sanfilippo F. Thermodynamics of two flavor QCD from imaginary chemical potentials. Phys Rev D, 2009, **80**: 014502. DOI: 10.1103/PhysRevD.80.014502
[33] Sasaki C, Friman B and Redlich K. Quark number fluctuations in a chiral model at finite baryon chemical potential. Phys Rev D, 2007, **75**: 054026. DOI: 10.1103/PhysRevD.75.054026
[34] Ferroni L and Koch V. Mean field approach to flavor susceptibilities with a vector interaction. Phys Rev C, 2011, **83**: 045205. DOI: 10.1103/PhysRevC.83.045205
[35] Tao C, Ma Y G, Zhang G Q, *et al*. Symmetry energy dependence of the pygmy and giant dipole resonances in an isospin dependent quantum molecular dynamics model. Nucl Sci Tech, 2013, **24**: 030502.
[36] Xie W J and Zhang F S. Probing the density dependence of the symmetry energy with central heavy ion collisions. Nucl Sci Tech, 2013, **24**: 050502.
[37] Zhang Y X, Li Z X, Zhao K, *et al*. Constraints on symmetry energy and n/p effective mass splitting with improved quantum molecular dynamics model. Nucl Sci Tech, 2013, **24**: 050503.
[38] Feng Z Q. Isospin splitting of nucleon effective mass and isospin effect in heavy-ion collisions. Nucl Sci Tech, 2013, **24**: 050504.
[39] Son T D and Stephanov A M. QCD at finite isospin density. Phys Rev Lett, 2001, **86**: 592–595. DOI: 10.1103/PhysRevLett.86.592
[40] Zhang Z and Liu Y X. Coupling of pion condensate, chiral condensate and Polyakov loop in an extended NJL model. Phys Rev C, 2007, **75**: 064910. DOI: 10.1103/PhysRevC.75.064910
[41] Zhang Z and Liu Y X. Two-flavor QCD phases and condensates at finite isospin chemical potential. Phys Rev C, 2007, **75**: 035201. DOI: 10.1103/PhysRevC.75.035201
[42] Shao G Y, Colonna M, Di Toro M, *et al*. Isoscalar-vector interaction and its influence on the hadron-quark phase transition. Nucl Sci Tech, 2013, **24**: 050523.